5.6A

Statistical-Dynamical Forecasts of Warm Season Rainfall over North America

Christopher A. Davis, David A. Ahijevich, Richard E. Carbone, Kevin W. Manning and John Tuttle
National Center for Atmospheric Research[1,2]

1. INTRODUCTION

Carbone et al. (2002) identified a coherence of warm-season, continental precipitation on time and space scales greatly exceeding those of individual convective systems, yet not associated with traveling synoptic-scale disturbances in any obvious way. We refer to the coherent rainfall patterns as "episodes" to draw a distinction between the largest and longest duration events and individual convective complexes (e.g. Laing and Fritsch, 2000). The time-space coherence of precipitation patterns is suggestive of intrinsic predictability associated with warm season rainfall. This result is especially significant because operational numerical models exhibit low skill both in deterministic prediction of rainfall and also in representation of the spatial pattern of diurnal pattern of rainfall over the continental U.S.

In this article, we will first review the evidence for coherence of rainfall events and the statistical properties of this coherence. We will then demonstrate the clear failure of today's state-of-the-art mesoscale numerical weather prediction (NWP) models to capture this coherence and even the very basic patterns associated with the diurnal cycle of continental convection. We will then suggest how the observed coherence can be used to construct probabilistic forecasts of rainfall which may be combined with numerical guidance to achieve a substantial improvement in warm-season rainfall prediction.

2. Hovmoller Diagrams of Rainfall

In order to simplify the depiction of warm season rainfall over the continental U.S., we adopt a time-longitude (or time-latitude) rendering of rainfall approximated from national radar composites produced by WSI corporation (the NOW*rad*^{TM} product). For time-longitude (Hovmoller) depictions, we average the derived rainfall over strips that are only 0.05^{o} in longitude and extend from 30^{o} N to 48^{o} N latitude. The time resolution is 15 minutes. By averaging meridionally, we accentuate the zonal propagating attributes of warm season rainfall, depicted for two selected 15-day periods in Fig. 1. The left panel illustrates typical late-spring and mid-summer rainfall patterns. In May, there is considerable synoptic-scale "control" of the rainfall patterns, with rain streaks confined to the envelopes of convective instability in the favorable phase of large-scale disturbances. In July (right panel) synoptic-scale transients become of secondary importance, conditional instability is widespread and the rainfall patterns are dominated by the diurnal cycle and propagating streaks that often span 1-2 days and cover zonal distances of 1000-2000 km.

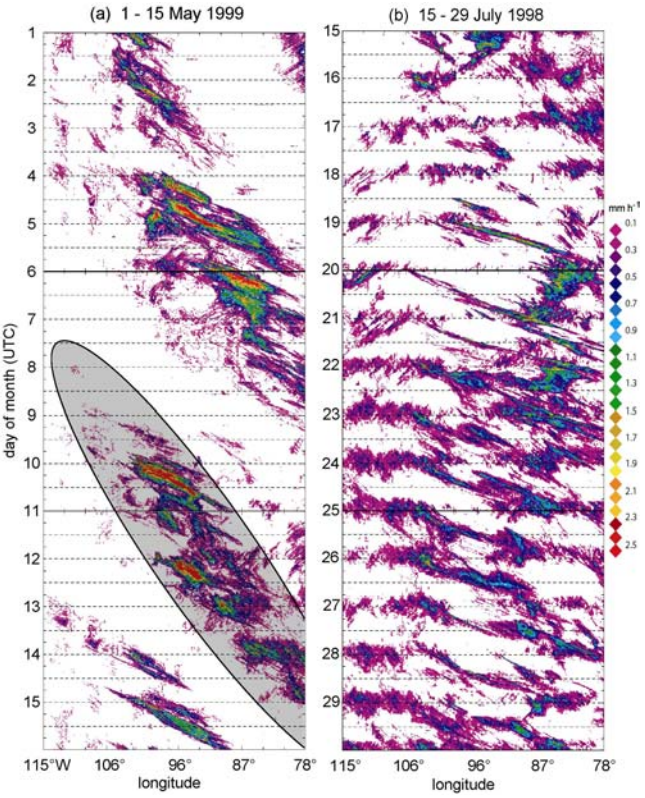

Figure 1. Radar-rainrate Hovmöller diagram for the period (a) 1-15 May 1999 and (b) 15-29 July, 1998. Panel (a) typifies spring conditions dominated by synoptic-scale transients wherein rain streaks are confined to precipitation "envelopes" (gray ellipse). Panel (b) typifies mid-summer conditions with a dominance of diurnal and propagating convection.

[1]The National Center for Atmospheric Research is sponsored by the National Science Foundation.

Corresponding Author:
Christopher A. Davis
P.O. Box 3000
Boulder, Colorado 80307
cdavis@ucar.edu

We have performed various calculations from the Hovmoller diagrams for the purpose of quantifying event coherency, longevity, zonal distance (hereinafter referred to as "span") and rate of propagation. Two-dimensional autocorrelation functions have been fit to the rainfall data in Hovmoller space. These functions define the coherent span, duration and propagation characteristics for each "rain streak," which is a time-longitude swath of rainfall. Most major episodes in Hovmoller space continuously produce at least some detectable precipitation throughout the episode duration. Coincidence errors (simultaneous events at different latitudes) occur in approximately 2% of all autocorrelation fits and have been manually corrected after review of the three dimensional data.

An additional set of Hovmoller diagrams, based upon the frequency of echoes at each UTC time/longitude coordinate, was created to examine the phase-locked behavior of precipitation echo at diurnal and higher frequencies. Every radar echo above ~15 dBZ_e constitutes an "event" at a longitude/time coordinate. The cumulative event frequency was averaged for monthly and seasonal periods as well as the entire 16-month period of record. An example depicting behavior during July, 1997 appears in Fig. 2. The diurnal cycle appears prominently around 80-90°W and 105°W. Also evident is a major propagation axis from 105°W to 92°W on day 1, and continuing from about 90°W to 80°W on day 2. The average apparent phase speed is about 14 m s^{-1}. There is weak evidence of continued eastward propagation on day 3, but it extends outside the area of good radar coverage. The diurnal and propagating features shown in Fig. 3 yield a distinct semi-diurnal signal of rainfall around 95°W.

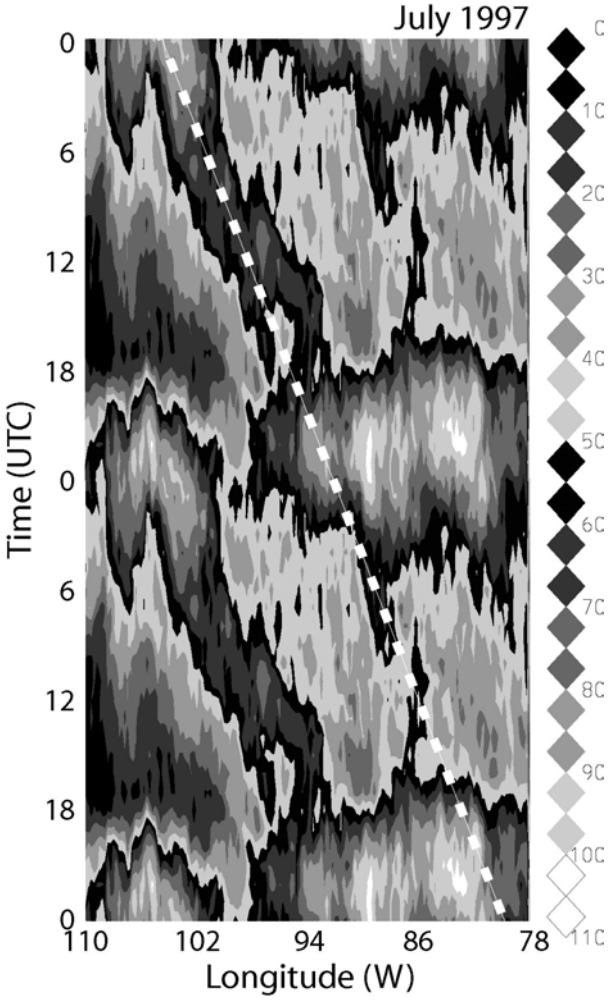

Figure 2. Occurrence frequency of latitudinally averaged reflectivity exceeding 15 dBZ as a function of longitude and time of day for July 1997. The diurnal cycle is repeated. The dashed white line represents a constant phase speed that connects day 1 and day 2 propagation.

The analyses and the statistics derived therefrom support the following conclusions:

- Coherent rainfall events, of order 1000 km in zonal span and one-day duration, occur with high frequency (nearly one per day).
- Such occurrences are believed to be *compound events*, a coherent succession of convective systems that appear causally related. We refer to these as "episodes."
- The steering level for the longer streaks averages near 400 hPa and is not a strong function of wind speed (i.e. propagation is additive to the wind).
- A significant portion of episodes exhibits phase-locked behavior, yielding signals in diurnal Hovmoller diagrams of (1) diurnal forcing over the eastern and western cordilleras and (2) semi-diurnal forcing between the cordilleras.

3. PERFORMANCE OF NWP MODELS

Given the diurnal and propagating signals of convection in the observations, it is reasonable to ask whether these signals are revealed in current NWP models. For this portion of the study, 3-hourly accumulated precipitation fields are examined for the Eta model (Black, 1994) from the National Centers for Environmental Prediction (NCEP) and for the Weather Research and Forecast model (WRF) (Michalakes et al. 2001). The Eta model precipitation from two forecasts per day is archived at NCAR as well as corresponding forecasts from the WRF model. Both models are run on a 22-km grid covering the continental U.S. The forecast length for all forecasts is 48 h. To avoid issues related to the spin-up of each model, we focus on the 12-36 h precipitation prediction.

Both Hovmoller and diurnal Hovmoller diagrams were constructed for the period July-August, 2001. The more revealing of these is the diurnal Hovmoller, here presented for only those forecasts initialized at 1200

UTC. To avoid the initial spinup of models, we use the 12-36 h forecast period to cover the diurnal cycle. We note that no qualitative differences result if 24-48 h forecasts are used.

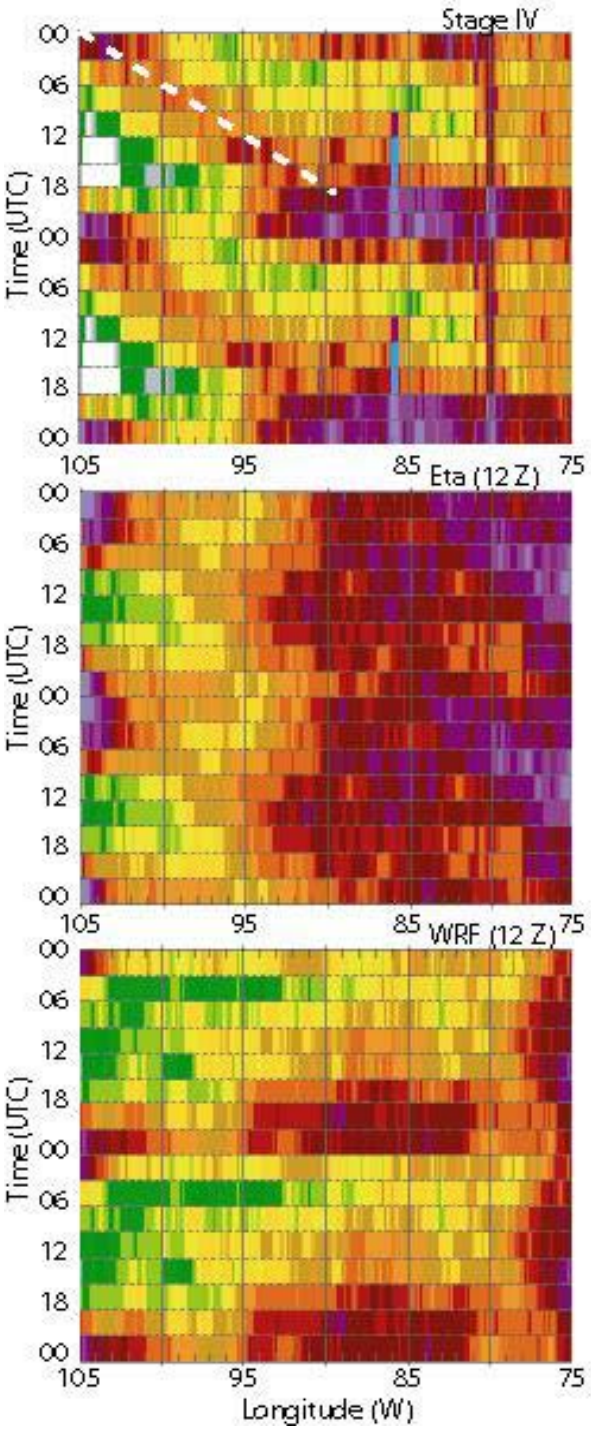

Figure 3. Diurnal Hovmöller diagrams of frequency of rainfall exceeding 1 mm averaged from 30-45°N within zonal strips of 10 km width covering the period July-August 2001. White dashed line highlights day 1 propagation axis. The diurnal cycle is repeated to more clearly show behavior near 00 UTC. Dark (purple) shading indicates high frequencies with a maximum of about 60%.White indicates less than 10%.

A convenient dataset for comparison is the Stage-IV precipitation analysis from NCEP, a combination of gauge- and calibrated radar-derived precipitation. As with the NOW*rad*^{TM} data, uncertainties in quantitative precipitation appearing in the NCEP analyses are likely substantial. Therefore, we will primarily compare patterns of precipitation rather than absolute amounts.

Three diurnal Hovmoller diagrams are shown in Fig. 3, corresponding to the NCEP analyses, WRF and Eta models, respectively. Several items are apparent:

- The primary day-1 propagation seen in Fig. 3 also appears in the NCEP analyses despite using 3-hourly data.
- The observed diurnal maximum near 85°W occurs around 2100 UTC; the maximum near the 105°W occurs near 0000 UTC, similar to Fig. 3
- Neither model correctly predicts the timing or longitude of most intense diurnal convection. The WRF model maintains a maximum between 90 and 95°W, with a maximum intensity occurring at about 1800 UTC, 3 hours early. The Eta exhibits virtually no diurnal cycle in convection east of 90°W.
- Neither model captures the primary propagation axis between about 104°W and 90°W. The WRF model exhibits no discernable propagation.

Notable errors in the diurnal cycle of convection in regional climate models were reported by Dai et al. (1999). Apparently, such first order errors are also a property of mesoscale models performing short-range forecasts. The large spatial and temporal errors of the diurnal cycle suggest that large-scale circulations, such as the mountain-plains solenoid, may be poorly handled. Uncertainties in the parameterization of deep convection are probably a key to the poor performance. Both models utilize the Betts-Miller cumulus parameterization, designed mainly for large-scale models. In traditional applications of this scheme, downdrafts are nearly absent. This could imply that one key to correctly predicting the propagation of convection across the Plains states is a realistic incorporation of downdraft physics.

4. STATISTICALLY-BASED PREDICTION

Because it is evident that forecast models currently are not able to faithfully reproduce the observed propagation characteristics of warm season rainfall, it is instructive to attempt probabilistic prediction based directly from the rainstreaks themselves. Eventually, a combination of empirical and NWP forecast techniques may provide the best overall predictions of warm season rainfall.

It turns out that the phase speed along individual streaks (of at least 6 h duration) is only slowly varying and can be calculated for individual streaks. Extrapolation of the rainfall streaks in time-longitude

space is possible if we know the statistics of streak duration, i.e., the probability that a given streak will continue for a certain number of hours.

We compute the probability of streak continuation from the entire 4-year sample (1997-2000), identifying all streaks beginning within contiguous 5^o by 5^o latitude-longitude boxes (Fig. 4). The number appearing within each box represents the number of streaks analyzed during the 4-year period. The duration probability exhibits a surprising amount of diurnal and longitudinal variation, with remarkably high probabilities of continuation for rain streaks emanating from the high plains during the early evening (up to 75%). Duration probabilities decrease for longer projections, but still exhibit similar spatial patterns.

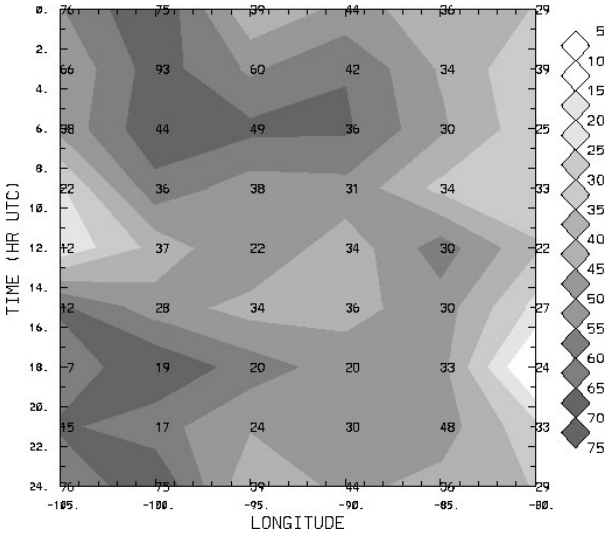

Figure 4. Probability (%) of a rain streak continuing for 6 h given that it has existed for 6 h, as a function of time of day (UTC) and longitude.

Given the probability of duration of rainfall streaks in time-longitude space, and given the variability of phase speeds over segments of individual streaks (typically about 3 m s^{-1}), one can construct probability contours in time-longitude space for the likelihood of streak passage through a particular time-longitude interval. In addition, a deterministic forecast of the end-point of a streak (again in time-longitude space) can be attempted by thresholding the duration probability.

5. DISCUSSION

Our findings contain inferences of predictability by reason of precipitation coherence patterns that exceed the dimensions of convective system lifecycles. Furthermore, the coherence properties are not "tightly held" by transient disturbances in the westerlies.

We have noted the almost complete absence of propagating signals from today's state-of-the-art NWP models and, in addition, a generally poor representation of the diurnal cycle of convection. These errors imply two things:

- The dynamics responsible for connecting individual mesoscale convective systems is virtually absent from NWP models.
- Statistically-based prediction of rainfall streaks may lend important information to augment numerical guidance of the timing and location of warm season rainfall.

Regarding the first point, it may be that higher resolution forecasts improve upon model performance by making models less reliant upon implicit precipitation schemes that have questionable relevance. Treatment of downdrafts and the resulting cold pool dynamics is often poor in models with grid spacing of 20 km or more.

We have suggested a simple way of using rain streaks and their statistics to provide probabilistic forecasts of warm-season rainfall from several to 24 h. Because this approach is based on the observed diurnal and propagating character of convection, and because these aspects are poorly treated in numerical models, it is possible that a combination of empirical (statistical) and dynamical (NWP) forecasts will provide better prediction of warm-season rainfall. The skill of the empirical method outlined herein, as well as strategies for combining it with numerical model guidance, will be presented at the conference.

ACKNOWLEDGEMENTS

This research was sponsored by National Science Foundation support to the U.S. Weather Research Program. The authors are deeply appreciative for assistance received from the National Climatic Data Center, the website of NOAA/CIRES Climate Diagnostics Center at U. of Colorado, S. Goodman of NASA's Marshall Spaceflight Center, NOAA/CIRA at Colorado State University, NOAA/NESDIS, and our sister organizations at NCAR/UCAR, namely the Research Applications Program and COMET. These organizations provided access to datasets critical to the analyses.

REFERENCES

Black, T. L., 1994: *Wea. and Forecasting*, **9**, 265-278.

Carbone et al., 2002: *J. Atmos. Sci.*, **59**, 2033-2056.

Dai, A., K. E. Trenberth, and T. R. Karl, 1999: *J. Geophys. Res.,* **104**, 6377-6402.

Liang and Fritsch, 2000: *Mon. Wea. Rev.,* **128**, 2756-2776.

Michalakes, J., S. Chen, J. Dudhia, L. Hart, J. Klemp, J. Middlecoff, and W. Skamarock, 2001: *Developments in Teracomputing*: Proceedings of the Ninth ECMWF Workshop on the Use of High Performance Computing in Meteorology. Eds, W. Zwieflhofer and N. Kreitz. World Scientific, Singapore. pp. 269-276.